



# Experimental and kinetic modeling study of ignition characteristics of RP-3 kerosene over low-to-high temperature ranges in a heated rapid compression machine and a heated shock tube

Yebing Mao, Liang Yu, Zhiyong Wu, Wencao Tao, Sixu Wang, Can Ruan, Lei Zhu, Xingcai Lu\*

*Key Laboratory for Power Machinery and Engineering of M. O. E., Shanghai Jiao Tong University, Shanghai 200240, PR China*



## ARTICLE INFO

### Article history:

Received 24 October 2018

Revised 7 December 2018

Accepted 13 February 2019

Available online 22 February 2019

### Keywords:

RP-3 kerosene

Ignition delay time

Surrogate fuel

Kinetic mechanism

Heated rapid compression machine

Heated shock tube

## ABSTRACT

Autoignition characteristics of RP-3 kerosene were investigated using a heated rapid compression machine and a heated shock tube over a wide range of conditions. Ignition delay times (IDTs) for RP-3 kerosene were measured at pressures of 10, 15 and 20 bar over a range of temperatures from 624 to 1437 K and for equivalence ratios from 0.5 to 1.5. A three-component surrogate fuel (49.8% dodecane, 21.6% iso-octane and 28.6% toluene by mole) was proposed and a kinetic model was developed to describe the combustion chemistry of RP-3. Negative temperature coefficient (NTC) behavior was observed in the autoignition, of which the temperature range varied within 701–884 K depending on operating conditions. IDT correlations in low and high temperature regions were obtained and then the dependences of IDT on pressure, equivalence ratio, oxygen content and dilution ratio were systematically studied. Comparison between the predictions using the new model and the experimental data shows that this model can accurately describe the autoignition characteristics of RP-3. Brute force sensitivity analyses were carried out to identify the key reactions that govern the ignition event. The large experimental data set and kinetic model provided in the current work will provide insights into the understanding of RP-3 ignition.

© 2019 The Combustion Institute. Published by Elsevier Inc. All rights reserved.

## 1. Introduction

Jet fuel accounts for a significant proportion of the liquid fuel consumption and is widely used to power aeroengines. A good understanding of the combustion chemistry of jet fuel is of significance for the development of aero-combustors. Chemical kinetic models describing the combustion chemistry of real fuel contain both surrogate fuels and kinetic mechanisms. The development of a high fidelity chemical kinetic model requires kinetic targets for validation, such as ignition delay times (IDTs). Except for being used to test and validate the kinetic mechanisms, IDTs can be used to evaluate the compatibility of the fuel with the engines as well, because undesirable autoignition in aeroengines must be avoided for safety reasons. Therefore, it is of great importance to investigate the autoignition characteristics of jet fuel.

The autoignition characteristics of jet fuels have been a subject of interest for many years. Efforts to measure IDTs of real jet fuel had been carried out by Mullins [1] as early as in the 1950s. Thereafter, many relevant studies have been done by researchers in various apparatus. Due to the high boiling point of large

molecular components, reactant mixtures usually reacted in the form of gas-liquid coexistence in the early IDT measurements for jet fuels. A detailed review of related publications prior to 2006 was provided by Dagaut and Cathonnet [2]. In the recent decade, beginning with the article of Dean et al. [3], gas-phase IDT measurement has become the preferred method in jet fuel relevant measurements since it can avoid the sedimentation and adsorption of droplets and provide more reliable and repeatable data. Among these measurements, important works are briefly reviewed as follows. Vasu et al. [4–6] measured IDTs for Jet-A and JP-8 at elevated pressures (17–51 atm) over a wide temperature range (715–1229 K) using heated shock tube (ST); Zhu et al. [7] report ST IDTs for JP-8, F-76 and a series of alternative fuels over a range of temperatures (1047–1520 K) and equivalence ratios (0.25–2.2); the experiments by Wang and Oehlschlaeger [8] were performed at high pressures (8–39 atm) in a wide temperature range (651–1381 K) at equivalence ratios from 0.25 to 1.5 and provided substantial IDT data for Jet-A POSF 4658; the study of Zhukov et al. [9] tested IDTs for Jet-A at pressures of 10 and 20 atm from 1040 to 1380 K at equivalence ratios 0.5, 1.0 and 2; Sung's group [10,11] and Lee's group [12–14] measured IDTs for Jet-A, JP8 and a series of alternative fuels at elevated pressure and low-to-intermediate temperature conditions using rapid compression machine (RCM); Dooley et al. [15,16] reported IDTs for stoichiometric Jet-A POSF 4658/air mixture at

\* Corresponding author.

E-mail address: [lyuxc@sjtu.edu.cn](mailto:lyuxc@sjtu.edu.cn) (X. Lu).

**Table 1**  
Comparison of composition between RP-3 and other jet fuels.

Fuel	n-alkanes (wt%)	Iso-alkanes (wt%)	Cycloalkanes (wt%)	Aromatics (wt%)	Molecular weight
RP-3	25.1	42.7	17.8	14.4	165 ( $C_{11.82}H_{23.20}$ )
Jet-A [20]	28	29	20	20	142
JP-8 [20]	19	38.2	24.1	13.5	153

645–1222 K and pressures around 20 atm by combining a heated ST and a heated RCM. Very recently IDT measurement of Jet-A-1 at low-to-high temperature was performed by De Toni et al. [17] using a heated ST and RCM; Burden et al. [18] reported IDTs of a series of conventional and alternative jet fuels from 1000 to 1400 K at pressures from 6 to 60 atm in a constant volume spray combustion chamber and ST. It must be noted that the above-mentioned studies mainly focused on Jet-A, JP-8, JP-5 and some alternative fuels. Compared with Jet-A and JP-8 etc., RP-3 is a different type of jet fuel with different composition and thus different combustion characteristic. Table 1 shows the comparison between RP-3 and Jet-A and JP-8. However, as one of the most important civil aviation fuels in China, RP-3 kerosene has received fewer attentions. To date, gas-phase IDT measurements for RP-3 are scarce, especially under low-to-intermediate temperature conditions. Zhang et al. [19] measured the IDTs of RP-3 using a heated ST at equivalence ratio of 0.2, 1.0 and 2.0, pressure of 1–20 atm. However, the experiments of Zhang et al. [19] mainly focused on high temperature conditions and seldom covered the low-to-intermediate temperature range (except for the stoichiometric mixture at 10 atm (651–1217 K)). It must be point out that even in high temperature range, IDT measurements for RP-3 were very limited compared with Jet-A and JP-8 etc.

It is of great importance to understand the combustion chemistry of low-to-intermediate temperature for RP-3. Firstly, low-T chemistry will affect the ignition reliability at cold start stage of engine. Furthermore, good knowledge of low-T IDTs of RP-3 is helpful to avoid premature ignition before fuel/air mixture reaches the main combustion zone. In recent years, there are some attempts to burn kerosene in internal combustion engines [21,22], which increasing the importance of low-T chemistry. Considering the great importance of low temperature chemistry, it is essential to develop reliable chemical kinetic mechanisms containing low-to-intermediate temperature reaction pathway for RP-3. However, the lack of experimental data, especially data in the low-to-intermediate temperature range, restricted the development of kinetic model for RP-3 somewhat. Up to date, there are only few kinetic models for this fuel. Zhang et al. [19] proposed a surrogate for RP-3 by referring to Aachen surrogate [23]. This surrogate fuel contains 88.7% n-decane and 11.3% 1,2,4-trimethylbenzene by mole, leading to a higher cetane number (CN) than RP-3. Zhang et al.'s model [19] was only validated against the high temperature IDTs and limited low temperature IDTs. Considering the higher CN of the surrogate fuel, there is a necessity to further validate this model against the data from more sources under wide conditions. Yu and Gou [24] formulated another surrogate fuel by matching functional groups and chemical structures and developed the corresponding chemical kinetic mechanism. However, this model was only validated against very limited experimental data. Therefore, there is an urgent need to obtain the IDTs for RP-3 over wide ranges and develop a detailed verified reaction mechanism for it.

The overarching goal of this study is to provide new reliable and comprehensive IDT data set and develop a kinetic model for RP-3. For this purpose, we measured the IDTs for this fuel over whole temperature ranges by combining a heated RCM and a heated ST. The measurements encompassing low to high temperature ranges (624–1437 K), pressures of 10, 15, and 20 bar and equivalence ratios from 0.5 to 1.5, were carried out. In addition, extreme di-

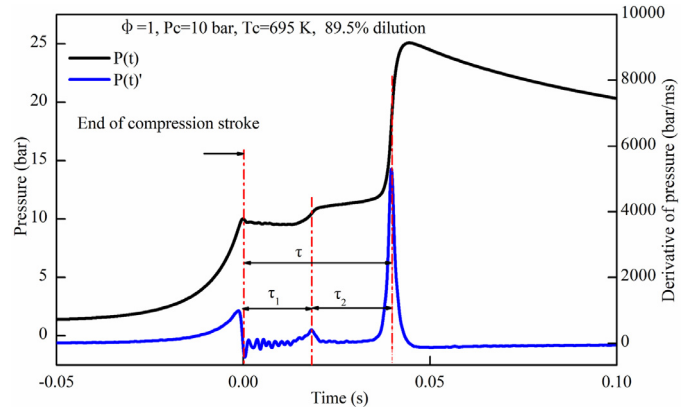


Fig. 1. Definition of IDT in RCM measurement.

lution conditions were also investigated. A three-component surrogate fuel was proposed and a modified mechanism (based on POLIMI\_kerosene\_231 mechanism [25]) was developed to model the autoignition behavior of RP-3.

## 2. Experimental methods

IDTs can be measured in several types of devices, among which RCM and ST are widely adopted. RCM is typically used to characterize the autoignition in low-to-intermediate temperatures due to the long experimental test durations, while ST is ideal devices for studying high temperature auto-ignition phenomena. In this study, a heated RCM and ST were combined to achieve IDT measurements over low-to-high temperature ranges.

### 2.1. Heated RCM

IDT measurements at low-to-intermediate temperature were carried out in the heated RCM at Shanghai Jiao Tong University (SJTU). The details of the heated RCM can be found elsewhere [26–29] and it is only briefly described here. The heated RCM is pneumatically-driven and its braking system is upgraded on the basis of the previous one [30,31] to achieve a faster compression stroke. The exterior of the combustion chamber, mixture tank and the manifold between them are wrapped with flexible heating jacket, whose temperature can be precisely controlled with an uncertainty of  $\pm 0.5$  K to keep the vaporized mixture and cylinder wall at the same temperature and prevent fuel condensation. The dynamic pressure signal is measured by a pressure transducer (Kistler 6125B) and amplified by a charge amplifier (Kistler 5015). IDT ( $\tau$ ) is defined as the interval between the end of the compression stroke and the time of maximum of derivative of the pressure versus time, which equals to the sum of first-stage IDT (FIDT,  $\tau_1$ ) and second-stage IDT (SIDT,  $\tau_2$ ), as shown in Fig. 1. The temperature  $T_C$  at the top dead center (TDC) can calculate according to 'adiabatic core assumption' [32] using Eq. (1):

$$\int_{T_0}^{T_C} \frac{\gamma}{\gamma - 1} \frac{dT}{T} = \ln \left[ \frac{P_C}{P_0} \right] \quad (1)$$

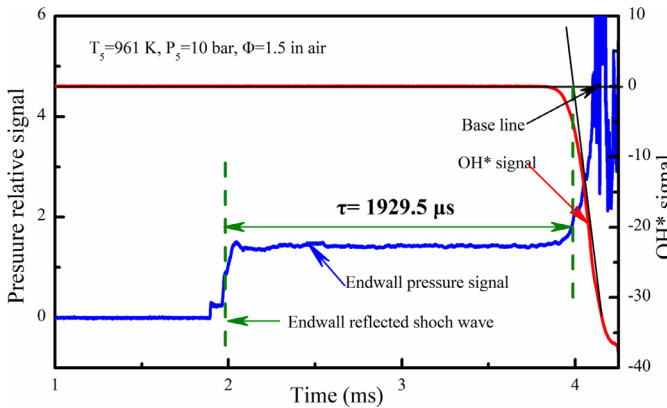


**Fig. 2.** Definition of IDT in ST measurement.

Where  $T_0$  is the initial temperature,  $\gamma$  the specific heat ratio, and  $P_C$  the measured pressure at TDC,  $P_0$  the initial pressure. The uncertainty of RCM measurement is mainly caused by the mixture preparation, measurement of pressure and the determination of temperature [27,33]. Taking all factors into account, the uncertainty of IDT in RCM is estimated to be less than  $\pm 10\%$  [27,33,34].

## 2.2. Heated ST

IDT measurements of RP-3 at high temperatures were performed in the heated ST at SJTU. The previous ST [35–37] was updated by adding the preheating system to enable the vaporization of large molecule fuels [38]. Flexible heating jackets were wrapped around the surface of the driven section and mixture tank, as well as manifold between them. Five pressure transducers (PCB113B26) were axially distributed at the last 0.76 m of the driven section evenly to record the arrival time of the incident shock wave and the reflected shock wave. The OH\* transition chemiluminescence passes through a 1.5 mm slit and focuses on the photomultiplier tube (Hamamatsu, R928) at the endwall of the driven section. In order to ensure consistency with literatures [35–40], the IDT ( $\tau$ ) in ST measurement is defined as the interval between the time of the reflected wave arriving at the endwall and the intercept of the maximum slope of the OH\* profile back to the baseline, as shown in Fig. 2. The temperature ( $T_5$ ) and pressure ( $P_5$ ) after the reflected shock wave were calculated using Gaseq [41]. The uncertainty of ST measurement is mainly caused by the determination of shock wave velocity and the maximum uncertainty is estimated to be  $\pm 20\%$  based on an Arrhenius-type correlation using the root-sum-squares (RSS) method, which was described in detail in [42,43].

## 2.3. Mixture preparation

The RP-3 sample used in the experiment is a complex mixture comprising of hundreds of hydrocarbons and its composition is determined by GC-MS analysis. Its composition is illustrated in Table 1 and other properties can be found in Table 3.

Mixtures of fuel/oxidizer were prepared in stainless steel mixture tanks heated to 140 °C. In order to control temperature with high accuracy, the temperatures of the mixture tank, manifold, the driven section of the heated ST or the combustion chamber of heated RCM, are maintained at the same value both in the RCM and ST experiments. Gaseous oxidizer and dilution gas were metered into the tank based on manometric basis while the fuel was injected into the tank based on mass basis. In order to ensure complete vaporization, the partial pressures of the major components in the tested fuel were limited to lower than half of their saturated vapor pressures at the preheating temperature. The monitoring results of fuel partial pressure showed that the vaporization

rate reached over 99.5% under all conditions. To ensure the complete vaporization and homogeneity, the mixtures were maintained at 140 °C for more than three hours before experiments. The purities of oxygen and nitrogen used in this experiment were 99.999%.

The test conditions are presented in Table 2. It must be noted that for RCM measurements, the non-reactive run was conducted by replacing the O<sub>2</sub> with an equal amount of N<sub>2</sub> for each test to emulate the heat loss during the compression stroke and the post-compression.

## 3. Kinetic modeling

### 3.1. Surrogate formulation

For multi-component complex mixture fuel, a suitable surrogate fuel is the prerequisite for modeling. In order to accurately describe the combustion behavior of RP-3, it is crucial to select appropriate target properties for formulating surrogate fuel. According to [16,44,45], lower heating value (LHV), CN, molecular weight (MW), hydrogen-carbon (H/C) ratio and threshold sooting index (TSI) are essential to duplicate the ignition and combustion behavior of real fuels. Hence, these five properties were selected as target properties. According to Dooley et al. [46], the role of naphthenic hydrocarbons can be replaced by isomeric alkanes in surrogate fuels. Hence, surrogate component candidates contain only three hydrocarbon classes, represented by n-dodecane, iso-octane and toluene, respectively. The composition was optimized through multivariate nonlinear programming by using the objective function given by Eq. (2) and a new surrogate fuel containing 49.8% n-dodecane, 21.6% iso-octane and 28.6% toluene was finally obtained.

$$F = \sum_{i=1}^M \left( \frac{p_{ic} - p_{it}}{p_{it}} \right)^2 * \omega_i \quad (2)$$

Where,  $p_{ic}$  is target property  $i$  of surrogate fuel,  $p_{it}$  is target property  $i$  of RP-3,  $\omega_i$  is the weight factor of property  $i$ , which was set to 1 in this study. For surrogate fuel, the target properties were calculated using the mixing rule listed in Table 3; for RP-3, TSI was estimated using the intermediate value (20) listed in Table 3 and the others were determined by measurements. The comparison of the target properties between surrogate fuel and real fuel was presented in Table 3.

### 3.2. Mechanism development

In the past decades, there are many sets of chemical mechanisms which were developed and validated for Jet-A and JP-8 surrogates, but fewer for RP-3. The mechanism developed by Ranzi et al. (POLIMI\_kerosene\_231 mechanism) [25] covers the reaction scheme of all the components used in the present surrogate fuel and thereby it is used as the onset of modeling.

The predictions of Ranzi's mechanism [25] were compared with the experimental data, as shown in Fig. 3. Note that all simulation in Fig. 3 are constant volume simulation. It can be seen in Fig. 3 that Ranzi's mechanism overestimates the IDTs by a factor of 3 in high-temperature (High-T) region; in addition, the predicted NTC temperature ranges is wider by about 40 K than experimental results. Sensitivity analysis at 1000 K showed that n-dodecane related reactions show highest sensitivities, indicating that the dodecane sub-mechanism are responsible for the discrepancy in this temperature range. The skeletal oxidation mechanisms for n-dodecane developed by Chang et al. [47] can well capture the existing IDTs of n-dodecane over low-to-high temperature ranges. In addition, Chang et al.'s n-dodecane skeletal mechanism was also adopted by Yu et al. [48] in their mechanism for Jet-A POSF-4658 and showed good predictive capacity. Therefore, the n-dodecane

**Table 2**  
Test conditions.

Equivalent ratio	$x_{\text{Fuel}}$ (mol%)	$x_{\text{O}_2}$ (mol%)	$x_{\text{N}_2}$ (mol%)	Dilution ratio $x_{\text{N}_2}/(x_{\text{N}_2}+x_{\text{O}_2})$	Pressure (bar)
0.5	0.59	20.88	78.53	79%	10/15
1.0	1.18	20.75	78.07	79%	10
1.5	1.76	20.63	77.61	79%	10
1.0	0.59	10.44	88.97	89.5%	10/15/20
1.5	0.59	6.96	92.45	93%	10/15/20

**Table 3**  
Target properties of RP-3 and that of the surrogate fuel estimated by mixing rule.

Target property	RP-3	RP-3 surrogate	Mixing rule of target properties
LHV	42.4	43.5	$\text{LHV} = \sum_{i=1}^N \text{LHV}_i * Y_i$ <sup>a</sup>
CN	43.3	43.99	$\text{CN} = \sum_{i=1}^N \text{CN}_i * V_i$ <sup>a</sup>
MW	165	159.75	$\text{MW} = \sum_{i=1}^N \text{MW}_i * X_i$ <sup>a</sup>
H/C	1.963	1.973	$\frac{\text{H}}{\text{C}} = \sum_{i=1}^N (\text{N}_{\text{Hi}} * X_i) / \sum_{i=1}^N (\text{N}_{\text{Ci}} * X_i)$ <sup>a</sup>
TSI	14-26 [45]	19.69	$\text{TSI} = \sum_{i=1}^N \text{TSI}_i * X_i$ <sup>a</sup>

<sup>a</sup> N-component number in the mixture,  $Y_i$  – mass fraction of component  $i$ ,  $V_i$  – volume fraction of component  $i$ ,  $X_i$  – mole fraction of component  $i$ ,  $N_{\text{Hi}}$  – hydrogen atom number in component  $i$ ,  $N_{\text{Ci}}$  – carbon atom number in component  $i$ .

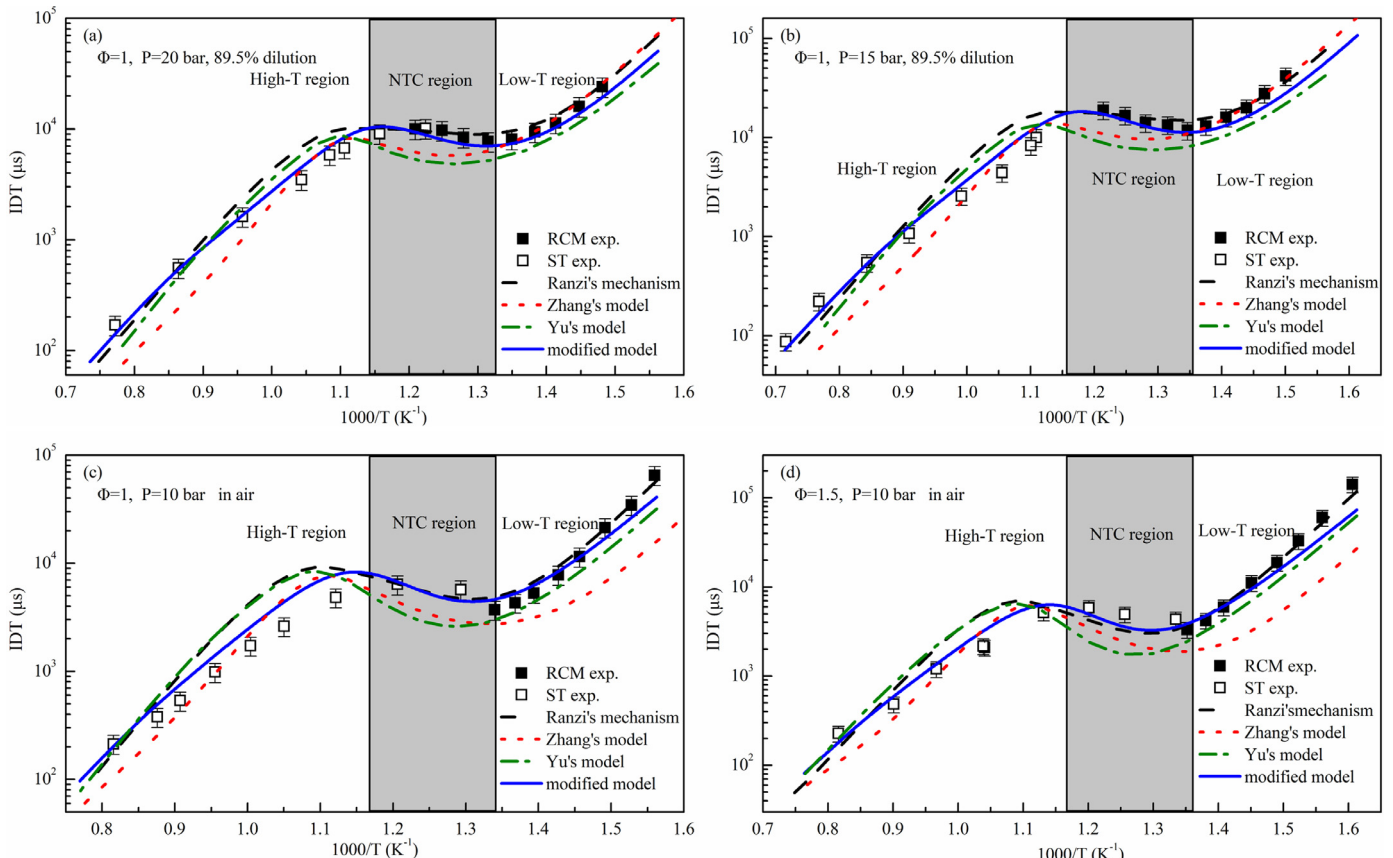


Fig. 3. Comparison of measured IDTs and prediction of kinetic models.

sub-mechanism of Ranzi's mechanism [25] was replaced by the n-dodecane sub-mechanism of Chang et al. [47], and a so-called modified model including 233 species and 5689 reactions was developed. It can be seen from Fig. 3 that the modified model shows obvious improved predictions in High-T region, while the predicted IDTs in Low-T and NTC region still maintain satisfactory agreements with the experimental results. Another obvious improvement is that the new model can accurately capture the NTC temperature ranges in all conditions.

The predictions of two published RP-3 kinetic models [19,24] (Table 4) are also presented in Fig. 3 to evaluate the

performance of the present model. In Fig. 3(a) and (b), Zhang's model [19] accurately predicts the IDTs in Low-T region for dilution mixture, however, it overestimated the reactivity in NTC and High-T region. In Fig. 3(c) and (d), however, Zhang's model [19] obviously overestimated the reactivity of the target fuel in Low-T region for fuel/air mixture. This can be attributed to the exorbitant content of n-alkane in Zhang et al.'s surrogate [19]. The exorbitant content of n-decane in surrogate leads to a greater CN than real RP-3. Since the CN is an indicative index of the reactivity of fuel, it is not surprising to observe the above discrepancy. Yu's model [24] can somewhat capture the variation trend of IDTs for RP-3,

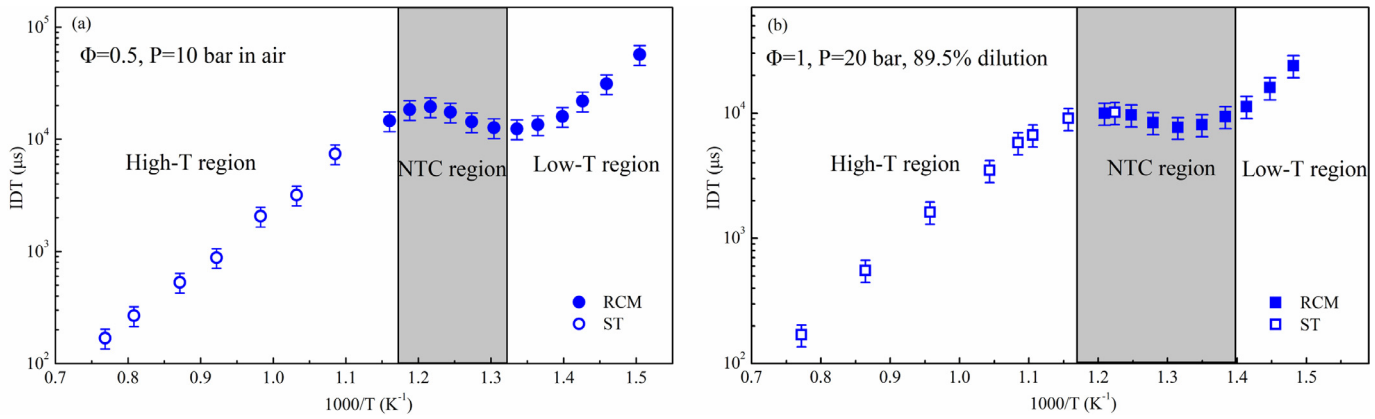


Fig. 4. Autoignition characteristics of RP-3 under typical conditions.

**Table 4**  
RP-3 surrogate fuels and their associated mechanisms used in the present study.

Model	Surrogate composition (by mole)	Kinetic mechanism
Zhang's model [19]	n-decane 88.7% 1,2,4-trimethylbenzene 11.3%	119 species and 527 reactions
Yu's model [24,49]	n-Dodecane 54.3% 2,5-dimethylhexane 32.1% Toluene 13.6%	373 species and 1763 reactions
Present model	Dodecane 49.76% Iso-octane 21.63% toluene 28.61%	223 species and 5689 reactions

but the predictions deviate from the experimental data to varying extents almost in all conditions. Compared with these models, the present model shows the closest agreement with the experimental data, especially in the NTC region. The validation against data in literature can be found in the supplemental material.

The simulation and analysis in the following sections were done with the constant-volume constraint using the modified model through Chemkin-Pro software; while for the RCM data, variable-volume simulations were also carried out with the 'effective volume' [50] to emulate the effect of heat loss during the compression stroke and post-compression on IDTs.

#### 4. Results and discussion

##### 4.1. Typical characteristics of RP-3 autoignition

Figure 4 presents the IDTs under two typical conditions to illustrate the autoignition characteristics of RP-3. As shown in Fig. 4, the RCM data and ST data are complementary in terms of the temperature range. Figure 4(a) and (b) show smooth transition over an entire temperature range at two different conditions. These two sets of data in Fig. 4 illustrate the good consistency between the ST and RCM results in the present work. Similar to other jet fuels such as Jet-A [8,10], RP-3 exhibits significant NTC behavior. However, the temperature range of NTC behavior changes as operating conditions are changed, e.g., from 749 to 822 K in Fig. 4(a) to 741 to 864 K in Fig. 4(b). Outside the NTC region, the variation of IDTs with temperature follows the Arrhenius law.

The pressure trace contains abundant information, which are helpful to understand the ignition characteristics of RP-3 and may be lost in the derived IDTs. Figure 5 shows parts of the pressure trace corresponding to RCM data in Fig. 4(a). The pressure trace begins to present an obvious double-stage ignition event at 685 K, including both the first-stage ignition and second-stage ignition. The first-stage ignition, also known as low temperature exothermic re-

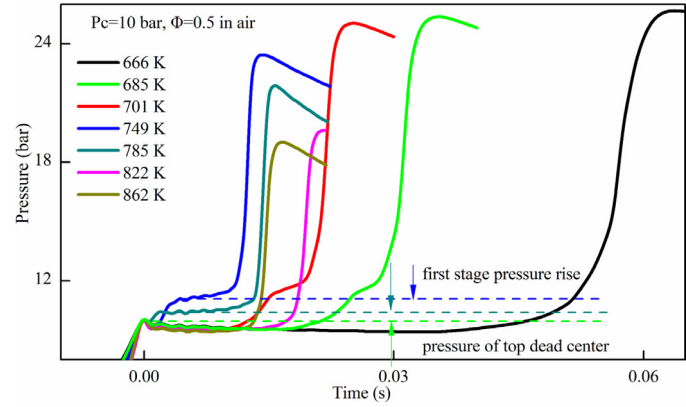
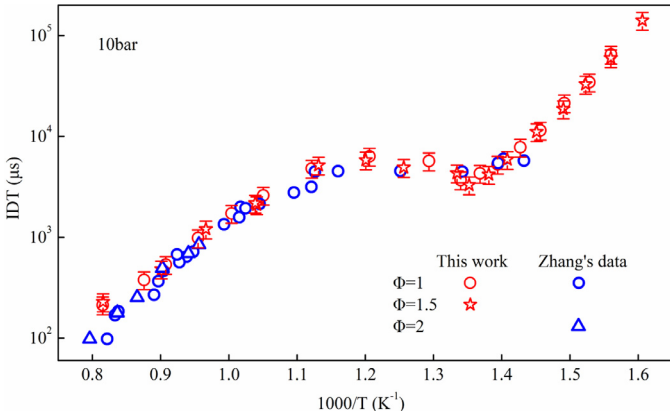


Fig. 5. Pressure trace under typical conditions.

actions or cool flame phenomenon, is usually characterized by a sharp rise in pressure [51–53]. Zhang et al. [54] and Liang and Law [55] reported the NTC behavior of FIDT for iso-octane and methylcyclohexane, however, similar behavior was not observed in RP-3 ignition. From 685 to 822 K in Fig. 5, FIDT decreases monotonously with temperature, while the SIDT increases monotonously. Hence, from the evolution trend of FIDT and SIDT, the single-stage ignition at 666 K may be a "pseudo" single-stage ignition with a very short SIDT hard to be detected. At 822 K or above, a single-stage ignition event is observed and the first-stage pressure rise disappeared. Since the competition between low temperature chain branching reaction sequence producing OH and the  $\beta$  scission of Low-T intermediates, there should be a critical initial temperature  $T^*$  (e.g. around 822 K in Fig. 5), above which the first-stage ignition will vanish, as stated by Ji et al. [56].

Since the FIDT decreases with the increase of initial temperature in Fig. 5, it can be concluded that the second-stage ignition dominates the NTC behavior of RP-3. The second stage ignition, also known as the main ignition event or High-T exothermic reaction, is closely related to the thermodynamic environment of the transition state from the first-stage ignition to the second-stage ignition, including the initial temperature  $T_2$ , pressure  $P_2$  and radical pool at the onset of second-stage ignition. According to Ji et al. [56] and Zhang et al. [54],  $T_2$  decreases with the increase of initial temperature. As shown in Fig. 5, the pressure rise  $\Delta P$  caused by the first-stage heat release decreases with the increase of initial temperature, leading to a lower  $P_2$ . The calculation of Zhang et al. [54] demonstrated that with increasing initial temperature less reactive species pool causes a significant decrease in the overall reactivity at the beginning of the second-stage ignition. In summary,



**Fig. 6.** Comparison with previous measurements of RP-3 [19].

the temperature, pressure and the radical pool at the beginning of the second-stage ignition decrease with the increase of the initial temperature when below  $T^*$  and thus SIDT increases. Above 822 K in Fig. 5, the Low-T pathway is suppressed, and a single-stage ignition occurs. Therefore, the total IDT is completely dependent on the state of the end of the compression stroke and decreases with increasing temperature, implying the occurrence of High-T region ignition.

#### 4.2. Comparison with literature data

In order to demonstrate the authenticity of our results, we compared them with previously available data. We selected the study of Zhang et al. [19] because it provided the opportunity to compare the data at similar experimental conditions. The comparison of the data is shown in Fig. 6. It can be found that the data of Zhang et al. [19] shows excellent agreement with the present measurement and almost all the data lies within the error bar. It must be pointed out that the data were obtained by two independent groups at different locations using different apparatus conducted again after several years, and hence the good agreement can demonstrate the reliability of the data.

Figure 7 further shows the comparison between the IDTs for RP-3 and other jet fuels, wherein Kumar's data, Allen's data and Zhu's data are scaled to 10 bar according the correlations provided by the authors [7,10,12]. In Fig. 7(a), It is observed that the ignition characteristics of RP-3 are quite different from Jet-A. Jet-A exhibits shorter IDTs in low and high temperature ranges and has an obviously different NTC behavior. Figure 7(b) present a comparison between RP-3 and JP-8. It can be seen that the general trend

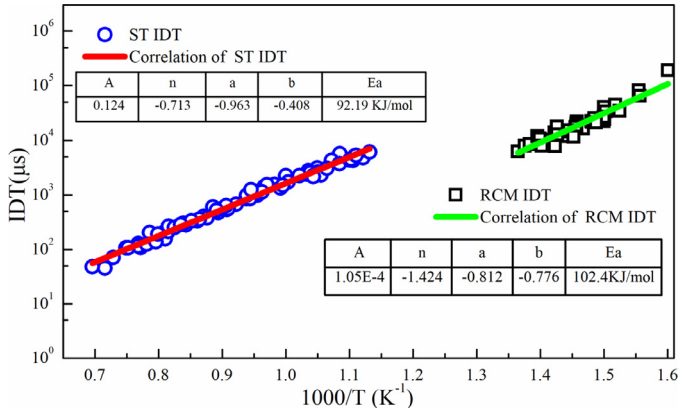


**Fig. 8.** Correlations of IDTs in high-T and low-T region (all data scaled to  $\Phi=1$ ,  $p=10$  bar).

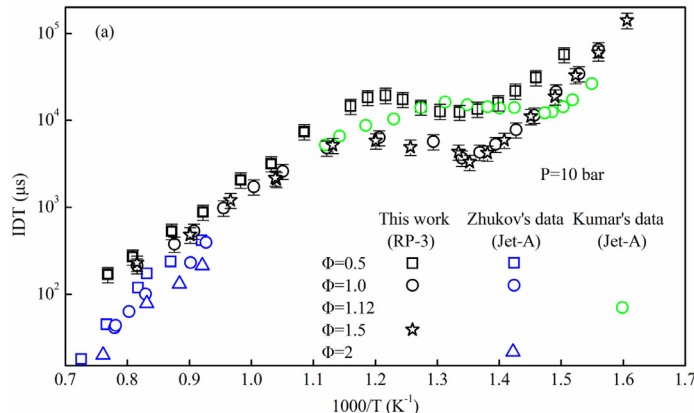
of the Arrhenius plots of RP-3 is similar to that of JP-8, however, RP-3 shows longer IDTs compared to JP-8. The discrepancy of the ignition characteristics suggests that the variation in the composition of fuel may affect the performance of engines and thus there is a necessity of studying the ignition characteristics of RP-3.

#### 4.3. Correlation of RP-3 IDTs

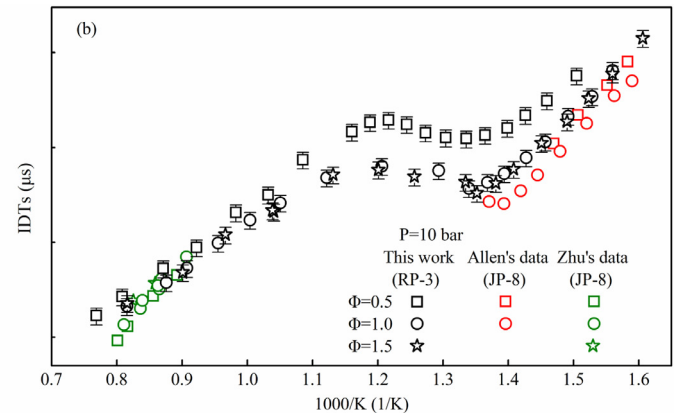
IDT correlation expressions are widely used for engine simulation and offer the opportunity to compare the results measured in different conditions. The correlation expressions provide a quantitative description of the effects of operating parameters on the ignition characteristics and can provide rough estimates when experimental data is unavailable. For ST data, the results usually must be scaled to the nominal pressure  $P_5$  according to the regression equation due to the difficulty in precisely controlling the pressure. Assuming IDTs in the High-T and Low-T regions is power-law dependence on the pressure, fuel mole fraction and oxygen mole fraction, and Arrhenius type dependence on temperature, correlation expressions can be described by Eq. (3):

$$\tau_{ign} = A \cdot P_c^n [\chi_{O_2}]^a [\chi_{Fuel}]^b \exp(E_a / RT_c) \quad (3)$$

Multiple linear regression analysis was performed for the data in the High-T and Low-T regions, respectively. The correlation results are shown in Fig. 8 with correlation coefficients  $R^2$  of 0.99 and 0.94, respectively (all data scaled to the condition of  $\Phi=1.0$  and 10 bar). Unlike the  $P^{-1}$  dependence for Jet-A observed in the literature [6], the  $P^{-0.71}$  dependence is found for IDTs in High-T region, indicating the weaker pressure dependence of RP-3. A



**Fig. 7.** Comparison of IDTs for RP-3 and Jet-A [7,9,10,12].



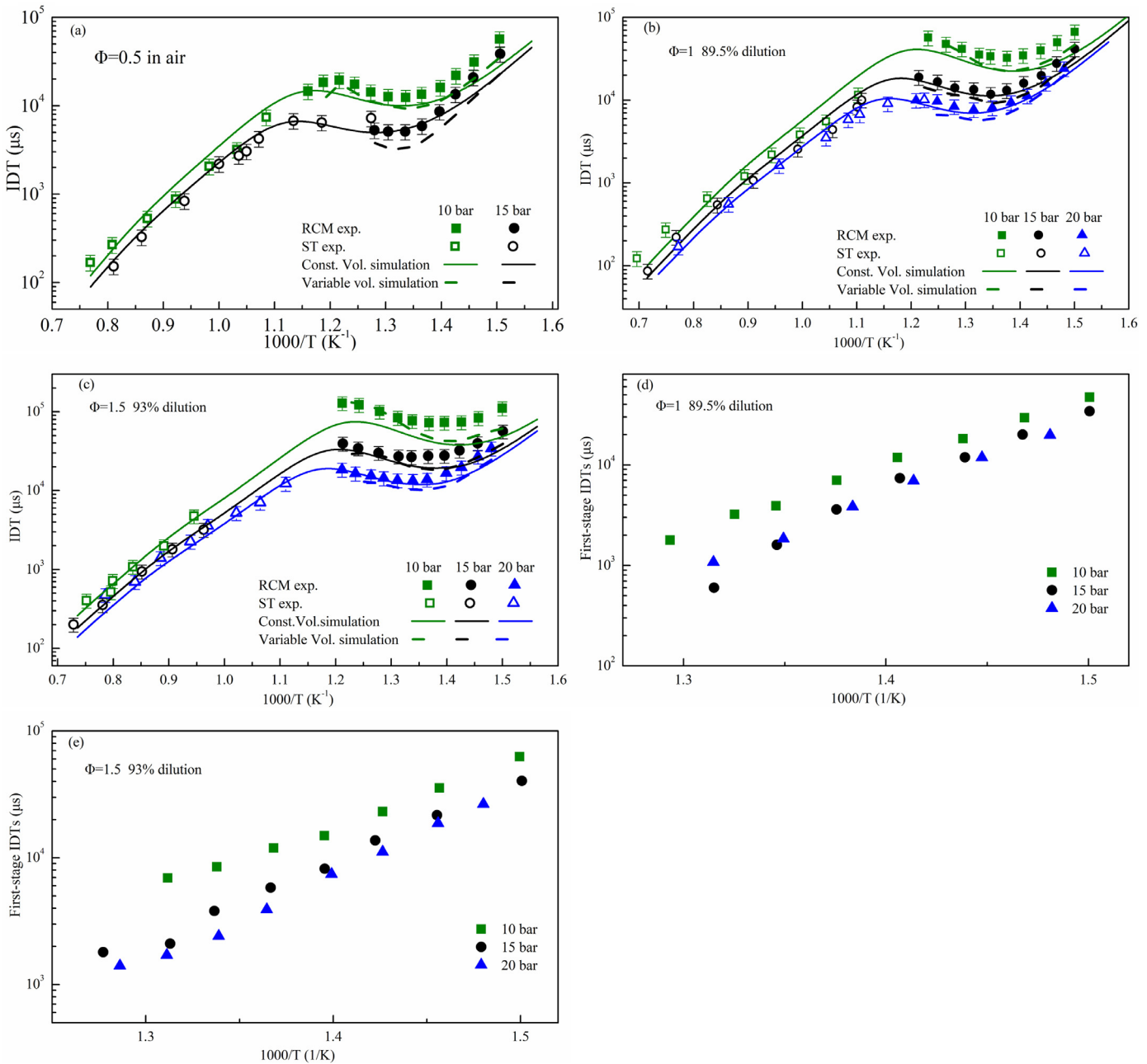


Fig. 9. Effect of pressure on IDTs of RP-3 under various equivalence ratio.

similar effect of pressure was also found in the study of Dean et al. ( $P^{-0.76}$ ) [3] and Zhukov et al. ( $P^{-0.67}$ ) [9]. Relatively speaking, IDTs in Low-T region show a stronger pressure dependence, and the dependence exponent ( $-1.42$ ) is very close to that of Jet-A ( $-1.39$ ) reported by Kumar et al. [10]. The effect of fuel mole fraction on IDTs in High-T region is quite different from that in the Low-T region. Specifically, the IDTs in Low-T region show much stronger dependence ( $-0.77$ ) on fuel mole fraction than in High-T region ( $-0.41$ ), due to the different reaction pathway. It is well known that High-T ignition is closely related to the chain branching reaction  $H + O_2 = OH + O$ . While for Low-T ignition event, fuel-dependent reactions, e.g., H abstraction from the fuel molecule and the oxygen addition steps forming  $RO_2$  and  $O_2QOOH$ , dominate the low-T chemistry. Therefore, the variation of fuel mole fraction has significant effect in the radical pool in Low-T region and thereby the effect on IDTs in Low-T region is more prominent. The temper-

ature dependences in the High-T and Low-T region are found to be similar.

In the later sections the ST data is normalized to the corresponding nominal pressure  $P_5$  according to Eq. (3) and the original data is provided in the supplemental material.

#### 4.4. Effect of operating conditions on IDTs

##### 4.4.1. Effect of pressure

Pressure dependence of IDTs has been an issue of interest and has been well studied for other hydrocarbons in literatures [9,57–61]. Figure 9 shows the effect of pressure at various equivalence ratios. As expected, for the shown equivalence ratios, IDTs decrease with the increasing pressure. For a given combustible mixture, higher pressure implies greater reactant concentration and higher collision probability, which inevitably increases the reaction inten-

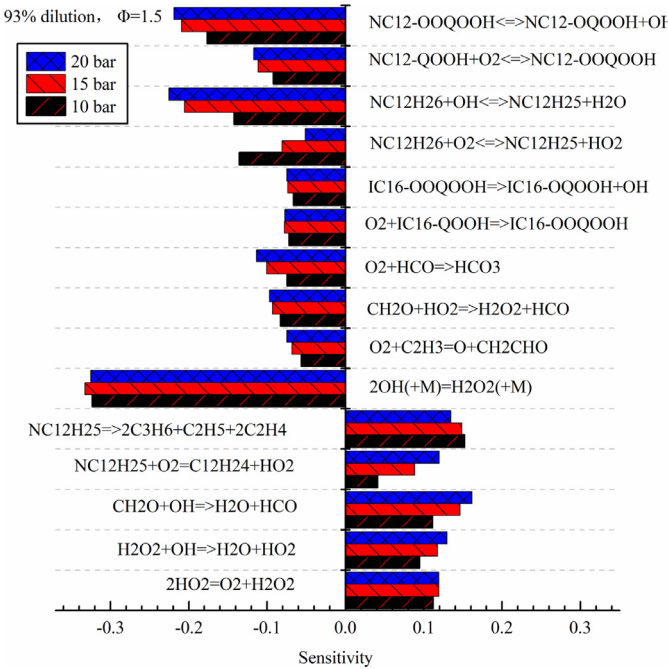


Fig. 10. Brute force sensitivity analysis for RP-3 at 800 K.

sity. It can be seen from Fig. 9 that the pressure dependence of the NTC region is most pronounced, while Low-T and High-T regions shows much weaker pressure dependence, which is very common in hydrocarbon fuels [8,29,51,62,63]. Figure 9 also shows both the constant volume and variable volume predictions of the modified model. It is found that the simulations are in good agreement with the experimental data. The model accurately captures the NTC behavior and pressure dependence of RP-3. The predictions in NTC and High-T region are basically within the experimental uncertainties. Brute force sensitivity analysis was carried out at 800 K under different pressures for 93% diluted reactive mixtures. The sensitivity is defined as:  $S_i = [\tau(2k_i) - \tau(k_i)]/\tau(k_i)$ . Wherein,  $k_i$  represents the rate constant of reaction  $i$ ,  $\tau(k_i)$  is the predicted IDT and  $\tau(2k_i)$  is the predicted IDT when the rate constant of reaction  $i$  is doubled. According to the definition, a negative sensitivity coefficient indicates a promotion effect on autoignition, whereas a positive one indicates the inhibition effect. The key reactions are illustrated in Fig. 10. Among these reactions, reaction  $2\text{OH} (+\text{M})=\text{H}_2\text{O}_2 (+\text{M})$  is pressure-dependent and shows the highest negative sensitivity in this temperature range. As pressure increases, the rate constant of this reaction increases quickly, leading to much shorter IDTs. Therefore, it can be concluded that the strongest pressure dependence in the NTC region may be related to this reaction. In addition, reactions of H abstraction from the fuel and OOQOOH isomerization to form keto-hydroperoxide and an OH radical are also very important reactions in NTC region. The starting temperatures of the NTC region of the three mixtures shown are found to shift to higher temperatures as pressure increases and less pronounced NTC behavior was observed at higher pressures. According to Al-Abbad et al. [62], this was caused by the increased stability of  $\text{RO}_2$  and faster decomposition of  $\text{H}_2\text{O}_2$  as pressure increases. Thus, the temperature at which ROO dissociation becomes competitive to ROO isomerization increases, transferring the NTC region to a higher temperature. However, for extreme dilution mixtures the prediction in the Low-T region is slightly lower than the experimental data, which will be considered in the future work.

The effect of pressure on FIDTs is displayed in Fig. 9(d) and (e). It can be seen that when pressure increases from 10 to 15 bar,

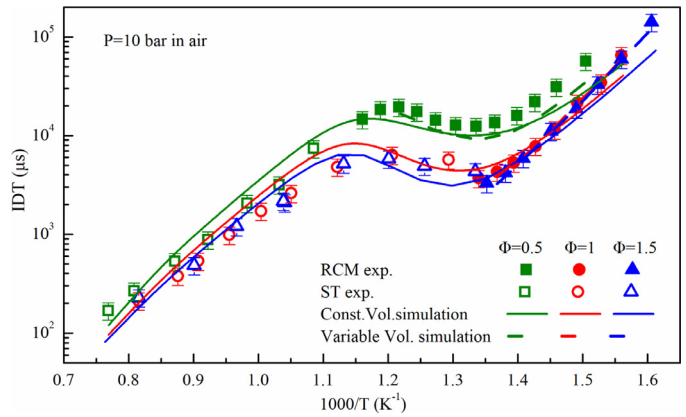


Fig. 11. Effect of equivalence ratio on IDTs of RP-3.

there is a slight decrease for FIDTs. In the study for Jet-A by Kumar and Sung [10], it is found that FIDTs show a reduction when pressure increased from 7 to 15 bar, which is consistent with the present study. However, when pressure increases from 15 to 20 bar, the FIDTs under the two pressures seem to be identical at similar temperatures, implying that FIDTs are insensitive to pressure. Similar trend was found in the studies of Mittal et al., Zhao et al. and Campbell et al. [64–66].

#### 4.4.2. Effect of equivalent ratio and oxygen mole fraction

Figure 11 shows a representative case for the effect of equivalence ratio for RP-3 at 10 bar. For the three shown conditions, the mole fractions of fuel were different while the mole fractions of oxygen remained basically constant (around 20.7%). Hence, the effect of equivalence ratio equates to the effect of fuel mole fraction here. As shown, the reactivity of the combustible mixture increases with the increase of the equivalence ratio. The equivalence ratio shows the strongest effect in NTC region. Brute force sensitivity analysis was carried out for different equivalence ratios in Low-T (700 K), NTC region (800 K) and High-T region (1350 K), as shown in Fig. 12. It can be seen from Fig. 12(a) that fuel consumption reactions (H abstraction from the fuel molecule by OH) and the formation of keto-hydroperoxide and OH through OOQOOH isomerization show the highest negative sensitivity at 700 K. In addition, the chain branching  $2\text{OH} (+\text{M})=\text{H}_2\text{O}_2 (+\text{M})$  following fuel consumption reaction ( $\text{RH}+\text{HO}_2=\text{R}+\text{H}_2\text{O}_2$ ) also plays a significant role in these temperature ranges. However, for the fuel-rich mixture, the sensitivity of  $2\text{OH} (+\text{M})=\text{H}_2\text{O}_2 (+\text{M})$  and H abstraction from the fuel molecule by OH ( $\text{NC}_{12}\text{H}_{26}+\text{OH}=\text{NC}_{12}\text{H}_{25}+\text{H}_2\text{O}$ ) reduced remarkably in the low-T region, as shown in Fig. 12(a). Therefore, equivalence ratio exhibits a much weaker effect for the fuel-rich mixture. While at 800 K, it can be found in Fig. 12(b) that the above-mentioned fuel-dependent reactions show higher negative sensitivity compared to at 700 K. This is the reason why IDTs show the strongest dependence on equivalence ratio in NTC region. It can be seen from Fig. 12(c) that the oxygen-dependent reaction  $\text{O}_2+\text{H}=\text{O}+\text{OH}$  shows the strongest negative sensitivity at 1350 K. In addition, the reactions of other small species also show strong sensitivity to the IDTs of RP-3. However, fuel-related reactions contribute less to promote the ignition. Therefore, the effect of equivalence ratio decreases compared to NTC region. The model accurately predicts this characteristic.

The effect of oxygen mole fraction is also investigated and the results are shown in Fig. 13. For the shown conditions, the fuel content was fixed at 0.59% and the equivalence ratio was adjusted by using three different oxygen contents: 20.87% ( $\Phi=0.5$ ), 10.44% ( $\Phi=1$ ) and 6.96% ( $\Phi=1.5$ ). Obviously, the in-

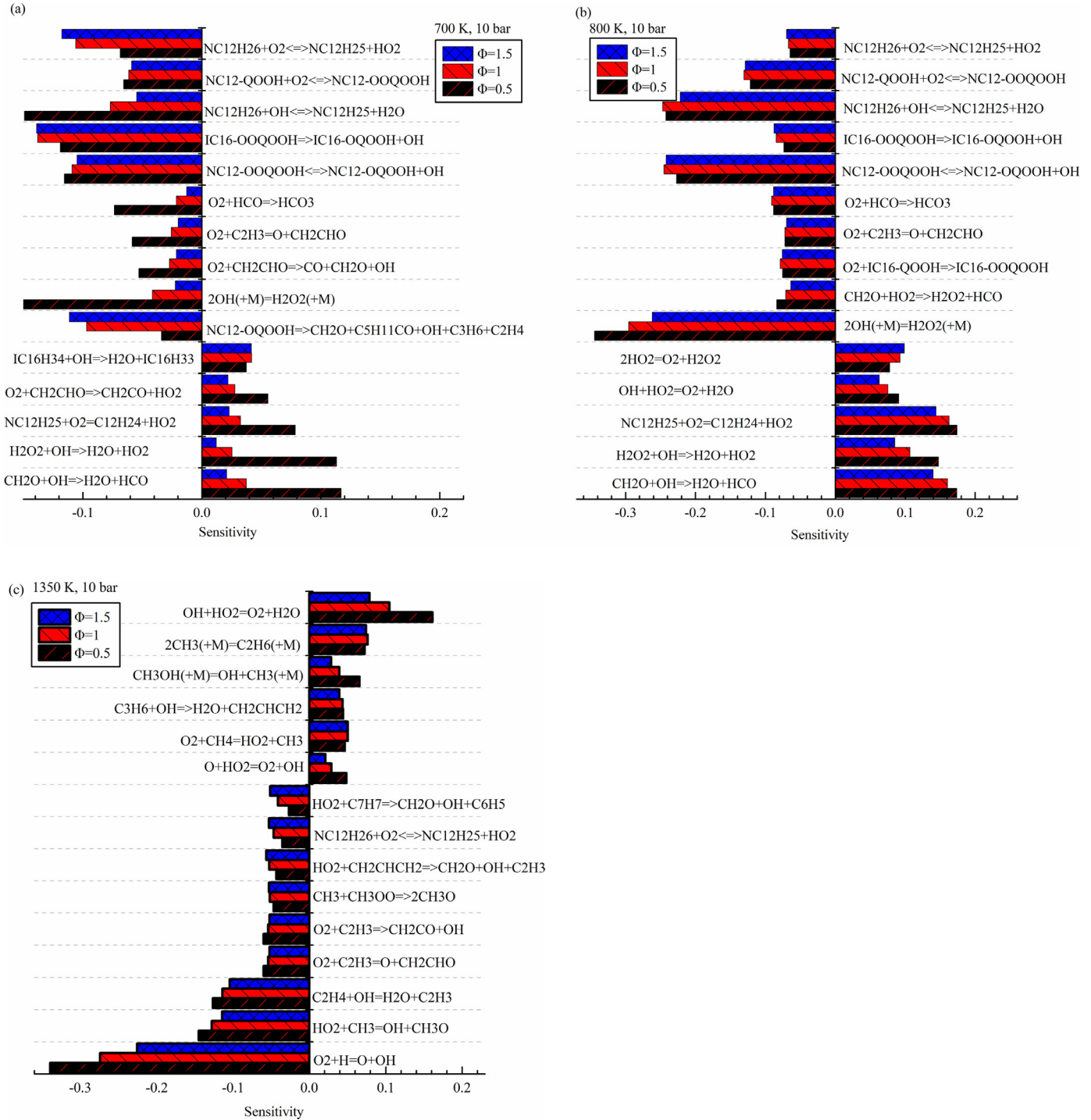
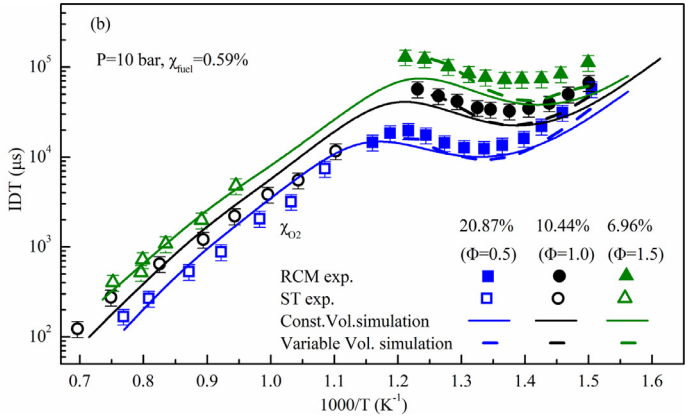
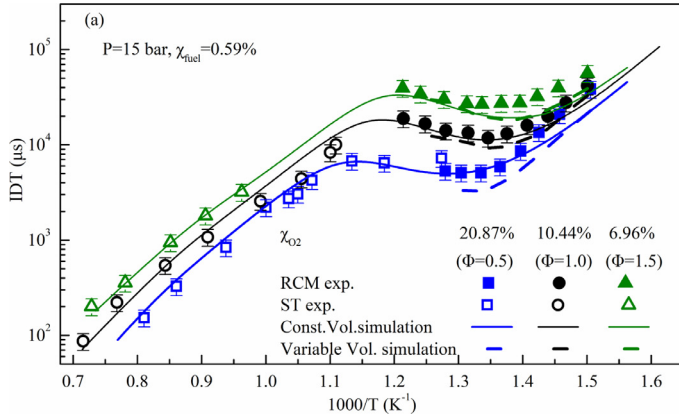


Fig. 12. Brute-force sensitivity analysis of IDTs performed for mixtures of different equivalence ratios.

crease of oxygen mole fraction can significantly increase the overall reactivity. As shown in Fig. 14, we found that the key reactions at low-to-intermediate temperatures include the chain-branching sequence of  $\text{O}_2$  addition steps (forming  $\text{O}_2\text{QOOH}$ ) and the consequence isomerization and decomposition. Therefore, at a constant fuel mole fraction, the oxygen content determines the overall reactivity. While for the High-T region, the dominant reaction  $\text{O}_2 + \text{H} \rightarrow \text{O} + \text{OH}$  is oxygen dependent. As a result, a stronger dependence on oxygen than pressure and fuel mole fraction was observed in the High-T region. In summary, the oxygen mole fraction controls the system reactivity over the full temperature ranges

We also noted, as shown in Fig. 14, that the competition between  $2\text{OH} + (\text{M}) \rightarrow \text{H}_2\text{O}_2 + (\text{M})$  and  $2\text{HO}_2 \rightarrow \text{O}_2 + \text{H}_2\text{O}_2$  become more effective as oxygen content decreases, leading to a decreased reactivity. It can be seen from Fig. 13 that the NTC behavior starts at a higher temperature and become less pronounced as oxygen content increases, which was well captured by the modified model. It should be noted that IDTs for the fuel-lean mixture and the fuel-rich mixture are both sensitive to oxygen mole fraction. Finally, we found that the oxygen content shows the strongest effect on IDTs in NTC region. The model fairly predicts the dependence of RP-3 IDTs on oxygen mole fraction.



**Fig. 13.** Effect of oxygen mole fraction on the IDTs of RP-3 under different pressures.

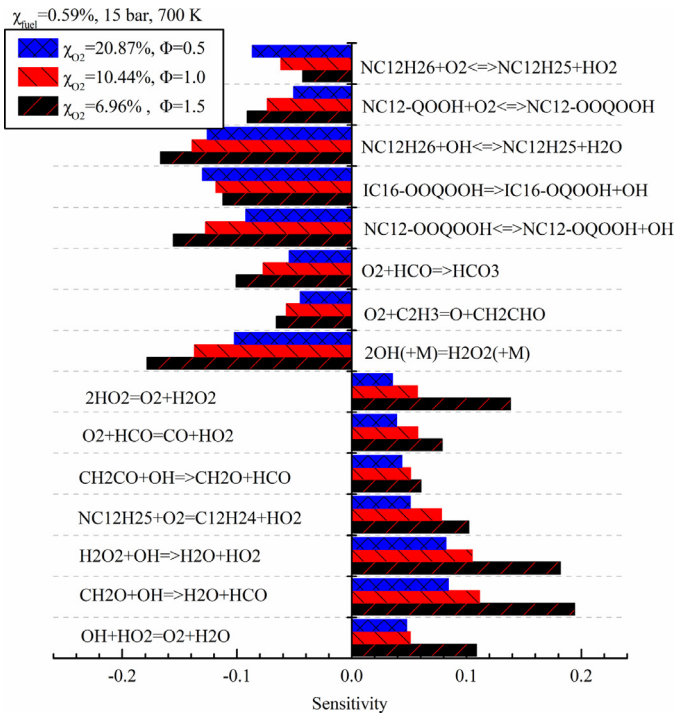


**Fig. 14.** Brute-force sensitivity analysis of IDTs performed at 700 K and 15 bar for mixtures of different oxygen content.

**Figure 15** further compares the FIDT under the corresponding conditions in **Fig. 13**. In **Fig. 15(a)**, FIDT decreases rapidly with the increase of oxygen mole fraction for the oxygen-lean mixture as expected; while in the oxygen-rich side, FIDT for the mixture of  $\Phi=0.5$  almost coincides with that for the mixture of  $\Phi=1$  over the experimental temperature range and thus the variation of IDTs is mainly caused by SIDT. A similar phenomenon is found at 10 bar in **Fig. 15(b)**. This implies that oxygen affects the ignition event for oxygen-rich mixture through different reaction pathway compared with the oxygen-lean mixture.

#### 4.4.3. Effect of dilution on IDTs

It is of great significance to study the ignition characteristics of fuel in extremely diluted conditions for the sake of the development of new combustion technologies with high efficiency and low emissions. **Figure 16** shows the IDTs of RP-3 at different dilution ratios. It can be seen from **Fig. 16(a)** and (b) that with the increase of dilution, IDTs increase significantly due to the decrease of reactant partial pressure. **Figure 16(c)** compares the ignition characteristic between mixtures with the same reactant partial pressure and equivalence ratio but different pressures and dilution ratios, where the partial pressures of fuel and oxygen were fixed at 0.12 bar and 2.08 bar and an equivalence ratio of 1 was adopted. It can be seen that the IDTs of 79% dilution mixture at 10 bar are shorter than that of 89.5% dilution mixture at 20 bar, implying that the thermal effect of increasing  $N_2$  overwhelms the pressure effect.

As shown in **Fig. 17**, the sensitivities of reactions playing an inhibiting role remarkably increased as dilution ratio increased and thus much longer IDTs were measured. Again, the strongest

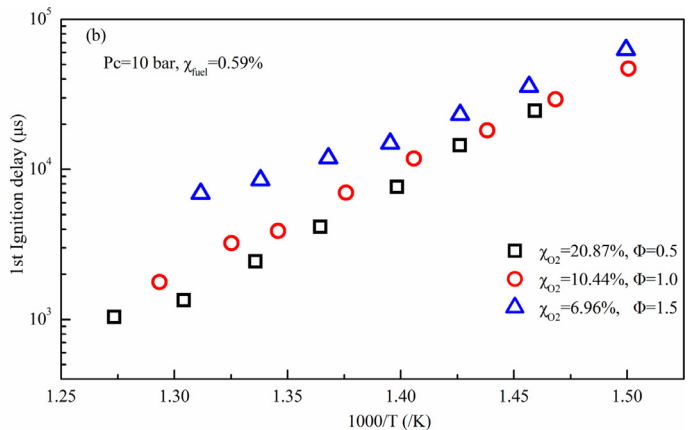
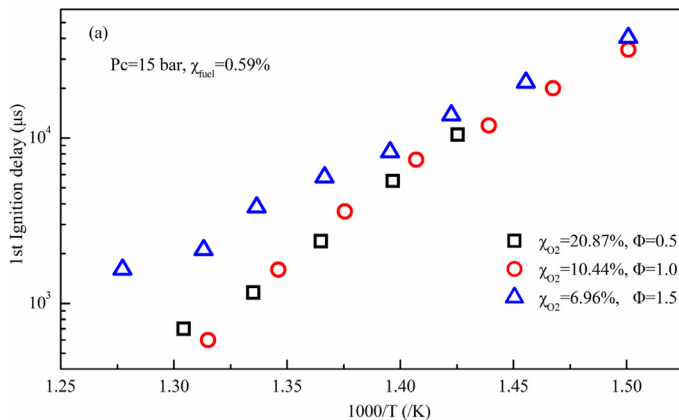


**Fig. 15.** Effect of oxygen mole fraction on FIDT of RP-3 under different pressures.

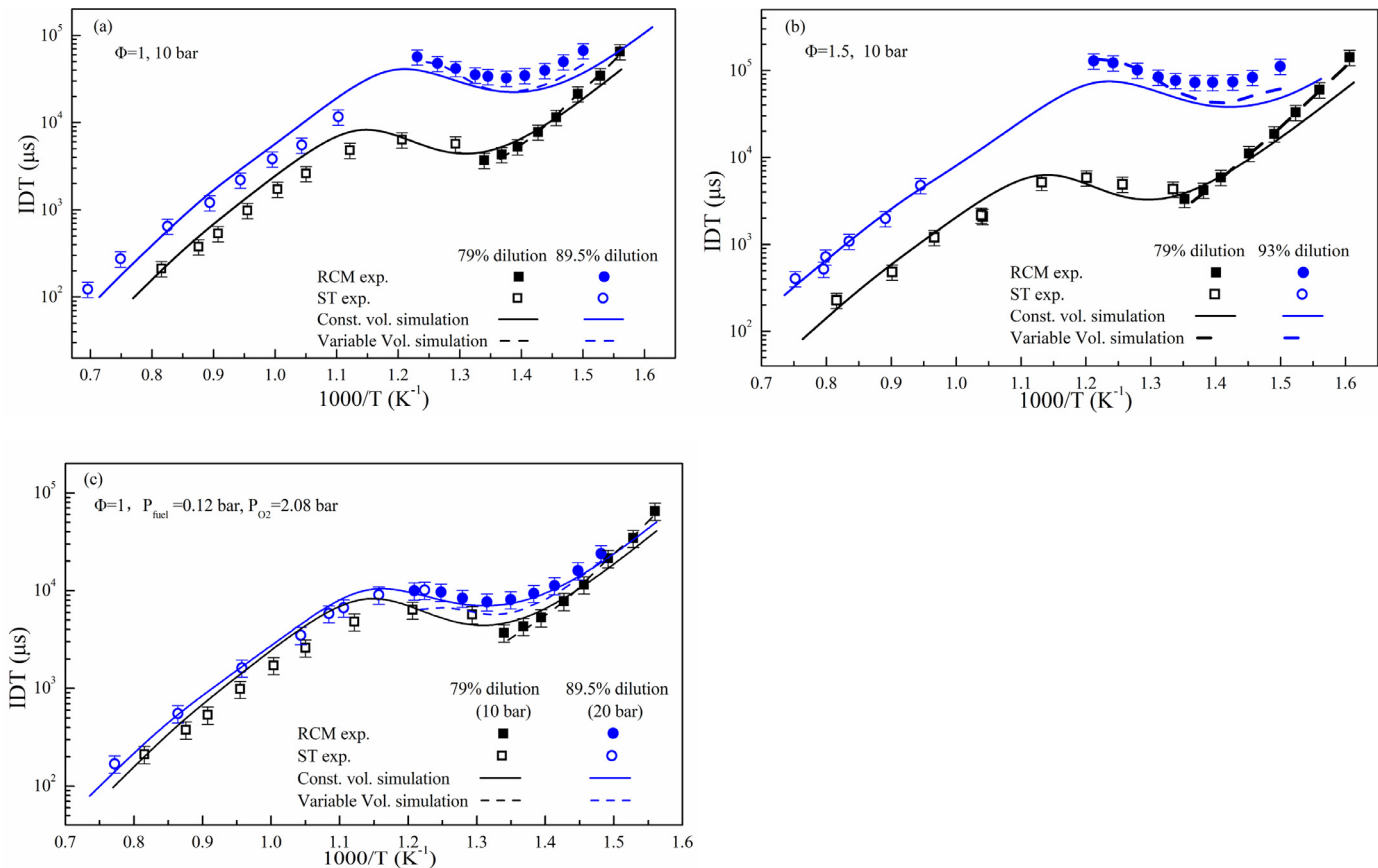


**Fig. 16.** Effect of dilution ratio on IDTs of RP-3.

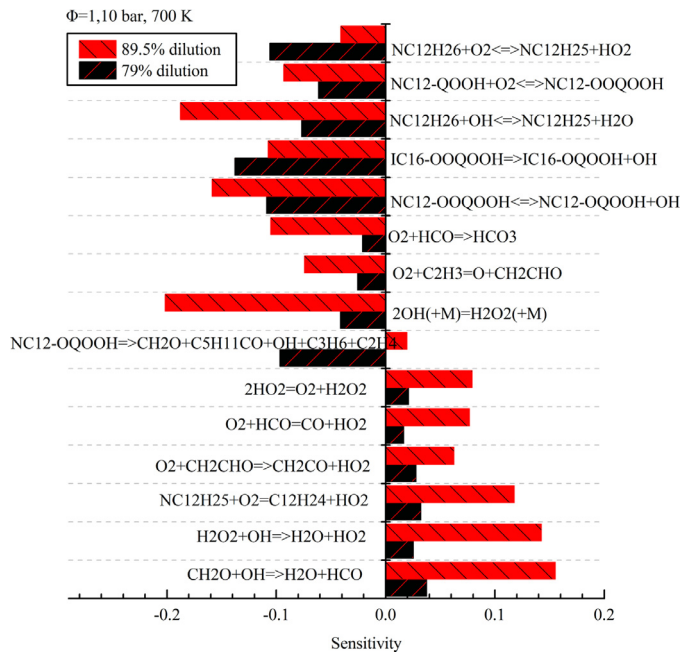


**Fig. 17.** Brute-force sensitivity analysis of IDTs performed at 700 K and 10 bar for mixtures of different dilution.

dependence on dilution ratio exists in the NTC region, just like other operating parameters. In addition, decreasing the dilution ratio leads to a shrunken NTC region, which is well captured by the modified model. However, the prediction under low

temperature for dilution mixtures needs to be improved. Reactions of  $\text{NC}_{12}\text{H}_{26} + \text{O}_2 \rightleftharpoons \text{NC}_{12}\text{H}_{25} + \text{HO}_2$ ,  $\text{NC}_{12}\text{H}_{26} + \text{OH} \rightleftharpoons \text{NC}_{12}\text{H}_{25} + \text{H}_2\text{O}$  and  $\text{NC}_{12}\text{H}_{25} + \text{O}_2 \rightleftharpoons \text{NC}_{12}\text{H}_{24} + \text{HO}_2$  exhibit strong sensitivity for diluted mixture while much weaker sensitivity for fuel/air mixture. Furthermore, products in these reactions are lumped species and, therefore, are the potential reactions for further mechanism optimization.

## 5. Conclusion

This study provides IDT data for RP-3 kerosene over a broad range of temperatures (624–1437 K), pressures (10, 15 and 20 bar) and equivalence ratios (0.5–1.5) by combining a heated ST and a heated RCM. The tested fuel exhibited obvious NTC behavior just like other jet fuels and variable NTC temperature ranges were observed under different operating conditions. Correlation expressions for IDTs in Low-T and High-T region were also provided in the present study. Based on the above work, the effects of pressure, equivalence ratio, oxygen mole fraction and dilution ratio on the IDTs were systematically analyzed. It is found that these parameters have the greatest impact on the IDTs in the NTC region, which may be related to the special reaction pathways in this temperature range. A three-component surrogate fuel containing 49.8% n-dodecane, 21.6% iso-cetane and 28.6% toluene by mole was proposed through matching five target properties including CN, MW, LHV, H/C and TSI. By updating the n-dodecane sub-mechanism, a new model containing 233 species and 5689 reactions was constructed for modeling RP-3. Comparison between the experimental data and predictions of the present model was made to evaluate the performance of the model. The results showed that this model can accurately describe the ignition characteristics of RP-3 since it

can accurately capture the variation trend of IDTs under all operating conditions and provide excellent agreeable IDT predictions. Finally, key reactions controlling autoignition and potential reactions for further model improvement were identified through brute force sensitivity analyses.

## Acknowledgment

The authors gratefully acknowledge the financial support from the Key Project of National Natural Science Foundation of China (No. 91641202, No. 51425602)

## Supplementary materials

Supplementary material associated with this article can be found, in the online version, at doi:10.1016/j.combustflame.2019.02.015.

## Reference

- [1] B.P. Mullins, Development of a combustion test rig for measuring the ignition delay of fuels, *Fuel* 32 (1953) 234–252.
- [2] P. Dagaut, M. Cathonet, The ignition, oxidation, and combustion of kerosene: a review of experimental and kinetic modeling, *Prog. Energy Combust. Sci.* 32 (2006) 48–92.
- [3] A.J. Dean, O.G. Penyazkov, K.L. Sevruk, B. Varatharajan, Autoignition of surrogate fuels at elevated temperatures and pressures, *Proc. Combust. Inst.* 31 (2007) 2481–2488.
- [4] S. Vasu, D. Davidson, R. Hanson, Shock Tube Ignition Delay Times and Modeling of Jet Fuel Mixtures, Paper AIAA-2006-4402, 2006.
- [5] S.S. Vasu, D.F. Davidson, R.K. Hanson, Jet Fuel Ignition Delay Times and Modeling: studies at High Pressures and Low Temperatures in a Shock Tube, Paper AIAA-2007-5671, 2007.
- [6] S.S. Vasu, D.F. Davidson, R.K. Hanson, Jet fuel ignition delay times: shock tube experiments over wide conditions and surrogate model predictions, *Combust. Flame* 152 (2008) 125–143.
- [7] Y. Zhu, S. Li, D.F. Davidson, R.K. Hanson, Ignition delay times of conventional and alternative fuels behind reflected shock waves, *Proc. Combust. Inst.* 35 (2015) 241–248.
- [8] H. Wang, M.A. Oehlschlaeger, Autoignition studies of conventional and Fischer-Tropsch jet fuels, *Fuel* 98 (2012) 249–258.
- [9] V.P. Zhukov, V.A. Sechenov, A.Y. Starikovskiy, Autoignition of kerosene (Jet-A)/air mixtures behind reflected shock waves, *Fuel* 126 (2014) 169–176.
- [10] K. Kumar, C.-J. Sung, An experimental study of the autoignition characteristics of conventional jet fuel/oxidizer mixtures: jet-A and JP-8, *Combust. Flame* 157 (2010) 676–685.
- [11] K. Kumar, C.-J. Sung, A comparative experimental study of the autoignition characteristics of alternative and conventional jet fuel/oxidizer mixtures, *Fuel* 89 (2010) 2853–2863.
- [12] C. Allen, D. Valco, E. Toulson, T. Edwards, T. Lee, Ignition behavior and surrogate modeling of JP-8 and of camelina and tallow hydrotreated renewable jet fuels at low temperatures, *Combust. Flame* 160 (2013) 232–239.
- [13] D. Valco, G. Gentz, C. Allen, M. Colket, T. Edwards, S. Gowdagiri, M.A. Oehlschlaeger, E. Toulson, T. Lee, Autoignition behavior of synthetic alternative jet fuels: an examination of chemical composition effects on ignition delays at low to intermediate temperatures, *Proc. Combust. Inst.* 35 (2015) 2983–2991.
- [14] D.J. Valco, K. Min, A. Oldani, T. Edwards, T. Lee, Low temperature autoignition of conventional jet fuels and surrogate jet fuels with targeted properties in a rapid compression machine, *Proc. Combust. Inst.* 36 (2017) 3687–3694.
- [15] S. Dooley, S.H. Won, M. Chaos, J. Heyne, Y. Ju, F.L. Dryer, K. Kumar, C.-J. Sung, H. Wang, M.A. Oehlschlaeger, R.J. Santoro, T.A. Litzinger, A jet fuel surrogate formulated by real fuel properties, *Combust. Flame* 157 (2010) 2333–2339.
- [16] S. Dooley, S.H. Won, J. Heyne, T.I. Farouk, Y. Ju, F.L. Dryer, K. Kumar, X. Hui, C.-J. Sung, H. Wang, M.A. Oehlschlaeger, V. Iyer, S. Iyer, T.A. Litzinger, R.J. Santoro, T. Malewicki, K. Brezinsky, The experimental evaluation of a methodology for surrogate fuel formulation to emulate gas phase combustion kinetic phenomena, *Combust. Flame* 159 (2012) 1444–1466.
- [17] A.R. De Toni, M. Werler, R.M. Hartmann, L.R. Cancino, R. Schießl, M. Fikri, C. Schulz, A.A.M. Oliveira, E.J. Oliveira, M.I. Rocha, Ignition delay times of Jet A-1 fuel: measurements in a high-pressure shock tube and a rapid compression machine, *Proc. Combust. Inst.* 36 (2017) 3695–3703.
- [18] S. Burden, A. Tekawade, M.A. Oehlschlaeger, Ignition delay times for jet and diesel fuels: constant volume spray and gas-phase shock tube measurements, *Fuel* 219 (2018) 312–319.
- [19] C. Zhang, B. Li, F. Rao, P. Li, X. Li, A shock tube study of the autoignition characteristics of RP-3 jet fuel, *Proc. Combust. Inst.* 35 (2015) 3151–3158.
- [20] C. Zhang, X. Hui, Y. Lin, C.-J. Sung, Recent development in studies of alternative jet fuel combustion: progress, challenges, and opportunities, *Renew. Sustain. Energy Rev.* 54 (2016) 120–138.
- [21] L. Chen, S. Ding, H. Liu, Y. Lu, Y. Li, A.P. Roskilly, Comparative study of combustion and emissions of kerosene (RP-3), kerosene-pentanol blends and diesel in a compression ignition engine, *Appl. Energy* 203 (2017) 91–100.
- [22] S. Gowdagiri, X.M. Cesari, M. Huang, M.A. Oehlschlaeger, A diesel engine study of conventional and alternative diesel and jet fuels: ignition and emissions characteristics, *Fuel* 136 (2014) 253–260.
- [23] S. Honnet, K. Seshadri, U. Niemann, N. Peters, A surrogate fuel for kerosene, *Proc. Combust. Inst.* 32 (2009) 485–492.
- [24] J. Yu, X. Gou, Comprehensive surrogate for emulating physical and kinetic properties of jet fuels, *J. Propuls. Power* 34 (2018) 679–689.
- [25] E. Ranzi, A. Frassoldati, A. Stagni, M. Pelucchi, A. Cuoci, T. Faravelli, Reduced kinetic schemes of complex reaction systems: fossil and biomass-derived transportation fuels, *Int. J. Chem. Kinet.* 46 (2014) 512–542.
- [26] S. Sun, L. Yu, S. Wang, Y. Mao, X. Lu, Experimental and kinetic modeling study on self-ignition of  $\alpha$ -methylnaphthalene in a heated rapid compression machine, *Energy Fuels* 31 (2017) 11304–11314.
- [27] L. Yu, Y. Mao, Y. Qiu, S. Wang, H. Li, W. Tao, Y. Qian, X. Lu, Experimental and modeling study of the autoignition characteristics of commercial diesel under engine-relevant conditions, *Proc. Combust. Inst.* 37 (2019) 4805–4812.
- [28] L. Yu, Y. Qiu, Y. Mao, S. Wang, C. Ruan, W. Tao, Y. Qian, X. Lu, A study on the low-to-intermediate temperature ignition delays of long chain branched paraffin: iso-cetane, *Proc. Combust. Inst.* 37 (2019) 631–638.
- [29] L. Yu, Z. Wu, Y. Qiu, Y. Qian, Y. Mao, X. Lu, Ignition delay times of decalin over low-to-intermediate temperature ranges: rapid compression machine measurement and modeling study, *Combust. Flame* 196 (2018) 160–173.
- [30] Z. Yang, Y. Qian, X. Yang, Y. Wang, Z. Huang, X. Lu, Autoignition of n-butanol/n-heptane blend fuels in a rapid compression machine under low-to-medium temperature ranges, *Energy Fuels* 27 (2013) 7800–7808.
- [31] Z. Yang, Y. Wang, X. Yang, Y. Qian, X. Lu, Z. Huang, Autoignition of butanol isomers/n-heptane blend fuels on a rapid compression machine in  $N_2/O_2/Ar$  mixtures, *Sci. China Technol. Sci.* 57 (2014) 461–470.
- [32] H. Hu, J. Keck, Autoignition of Adiabatically Compressed Combustible Gas Mixtures, SAE Technical Paper, (1987) 872110.
- [33] C.-J. Sung, H.J. Curran, Using rapid compression machines for chemical kinetics studies, *Prog. Energy Combust. Sci.* 44 (2014) 1–18.
- [34] H. Nakamura, D. Darcy, M. Mehl, C.J. Tobin, W.K. Metcalfe, W.J. Pitz, C.K. Westbrook, H.J. Curran, An experimental and modeling study of shock tube and rapid compression machine ignition of n-butylbenzene/air mixtures, *Combust. Flame* 161 (2014) 49–64.
- [35] H. Li, Y. Qiu, Z. Wu, S. Wang, X. Lu, Z. Huang, Ignition delay of diisobutylene-containing multicomponent gasoline surrogates: shock tube measurements and modeling study, *Fuel* 235 (2019) 1387–1399.
- [36] H. Li, L. Yu, X. Lu, L. Ouyang, S. Sun, Z. Huang, Autoignition of ternary blends for gasoline surrogate at wide temperature ranges and at elevated pressure: shock tube measurements and detailed kinetic modeling, *Fuel* 181 (2016) 916–925.
- [37] H. Li, L. Yu, S. Sun, S. Wang, X. Lu, Z. Huang, A shock tube experimental and modeling study of multicomponent gasoline surrogates diluted with exhaust gas recirculation, *Energy Fuels* 32 (2018) 3800–3813.
- [38] S. Wang, L. Yu, Z. Wu, Y. Mao, H. Li, Y. Qian, L. Zhu, X. Lu, Gas-phase autoignition of diesel/gasoline blends over wide temperature and pressure in heated shock tube and rapid compression machine, *Combust. Flame* 201 (2019) 264–275.
- [39] Z. Geng, L. Xu, H. Li, J. Wang, Z. Huang, X. Lu, Shock tube measurements and modeling study on the ignition delay times of n-butanol/dimethyl ether mixtures, *Energy Fuels* 28 (2014) 4206–4215.
- [40] L. Xu, L. Ouyang, Z. Geng, H. Li, Z. Huang, X. Lu, Experimental and kinetic study on ignition delay times of liquified petroleum gas/dimethyl ether blends in a shock tube, *Energy Fuels* 28 (2014) 7168–7177.
- [41] Gaseq. <http://www.gaseq.co.uk/> (Accessed 27 May 2018).
- [42] E. Hu, G. Yin, Z. Gao, Y. Liu, J. Ku, Z. Huang, Experimental and kinetic modeling study on 2,4,4-trimethyl-1-pentene ignition behind reflected shock waves, *Fuel* 195 (2017) 97–104.
- [43] Y. Li, C.-W. Zhou, H.J. Curran, An extensive experimental and modeling study of 1-butene oxidation, *Combust. Flame* 181 (2017) 198–213.
- [44] D. Kim, J. Martz, A. Violi, A surrogate for emulating the physical and chemical properties of conventional jet fuel, *Combust. Flame* 161 (2014) 1489–1498.
- [45] K. Narayanaswamy, H. Pitsch, P. Pepiot, A component library framework for deriving kinetic mechanisms for multi-component fuel surrogates: application for jet fuel surrogates, *Combust. Flame* 165 (2016) 288–309.
- [46] S. Dooley, J. Heyne, S.H. Won, P. Dievart, Y. Ju, F.L. Dryer, Importance of a cycloalkane functionality in the oxidation of a real fuel, *Energy Fuels* 28 (2014) 7649–7661.
- [47] Y. Chang, M. Jia, Y. Liu, Y. Li, M. Xie, H. Yin, Application of a decoupling methodology for development of skeletal oxidation mechanisms for heavy n-alkanes from n-octane to n-hexadecane, *Energy Fuels* 27 (2013) 3467–3479.
- [48] W. Yu, W. Yang, K. Tay, F. Zhao, An optimization method for formulating model-based jet fuel surrogate by emulating physical, gas phase chemical properties and threshold sooting index (TSI) of real jet fuel under engine relevant conditions, *Combust. Flame* 193 (2018) 192–217.
- [49] J. Yu, Z.J. Wang, X.F. Zhuo, W. Wang, X.L. Gou, Surrogate definition and chemical kinetic modeling for two different jet aviation fuels, *Energy Fuels* 30 (2016) 1375–1382.

- [50] S. Tanaka, F. Ayala, J.C. Keck, A reduced chemical kinetic model for HCCI combustion of primary reference fuels in a rapid compression machine, *Combust. Flame* 133 (2003) 467–481.
- [51] H.K. Ciezki, G. Adomeit, Shock-tube investigation of self-ignition of n-heptane-air mixtures under engine relevant conditions, *Combust. Flame* 93 (1993) 421–433.
- [52] S.S. Goldsborough, J. Santner, D. Kang, A. Fridlyand, T. Rockstroh, M.C. Jespersen, Heat release analysis for rapid compression machines: challenges and opportunities, *Proc. Combust. Inst.* 37 (2019) 603–611.
- [53] V.P. Zhukov, About kinetic modelling of n-decane autoignition, *Combust. Flame* 156 (2009) 1674–1676.
- [54] P. Zhang, W. Ji, T. He, X. He, Z. Wang, B. Yang, C.K. Law, First-stage ignition delay in the negative temperature coefficient behavior: experiment and simulation, *Combust. Flame* 167 (2016) 14–23.
- [55] W. Liang, C.K. Law, Theory of first-stage ignition delay in hydrocarbon NTC chemistry, *Combust. Flame* 188 (2018) 162–169.
- [56] W. Ji, P. Zhao, P. Zhang, Z. Ren, X. He, C.K. Law, On the crossover temperature and lower turnover state in the NTC regime, *Proc. Combust. Inst.* 36 (2017) 343–353.
- [57] V.P. Zhukov, V.A. Sechenov, A.Y. Starikovskii, Spontaneous ignition of methane-air mixtures in a wide range of pressures, *Combust. Explos. Shock Waves* 39 (2003) 487–495.
- [58] V.P. Zhukov, V.A. Sechenov, A.Y. Starikovskii, Ignition delay times in lean n-hexane-air mixture at high pressures, *Combust. Flame* 136 (2004) 257–259.
- [59] V.P. Zhukov, V.A. Sechenov, A.Y. Starikovskii, Self-ignition of a lean mixture of n-pentane and air over a wide range of pressures, *Combust. Flame* 140 (2005) 196–203.
- [60] V.P. Zhukov, V.A. Sechenov, A.Y. Starikovskii, Autoignition of a lean propane-air mixture at high pressures, *Kinet. Catal.* 46 (2005) 319–327.
- [61] V.P. Zhukov, V.A. Sechenov, A.Y. Starikovskii, Autoignition of n-decane at high pressure, *Combust. Flame* 153 (2008) 130–136.
- [62] M. AlAbbad, T. Javed, F. Khaled, J. Badra, A. Farooq, Ignition delay time measurements of primary reference fuel blends, *Combust. Flame* 178 (2017) 205–216.
- [63] R. Minetti, M. Carlier, M. Ribaucour, E. Therssen, L.R. Sochet, A rapid compression machine investigation of oxidation and auto-ignition of n-heptane: measurements and modeling, *Combust. Flame* 102 (1995) 298–309.
- [64] G. Mittal, M. Chaos, C.-J. Sung, F.L. Dryer, Dimethyl ether autoignition in a rapid compression machine: experiments and chemical kinetic modeling, *Fuel Process. Technol.* 89 (2008) 1244–1254.
- [65] P. Zhao, C.K. Law, The role of global and detailed kinetics in the first-stage ignition delay in NTC-affected phenomena, *Combust. Flame* 160 (2013) 2352–2358.
- [66] M.F. Campbell, S. Wang, C.S. Goldenstein, R.M. Spearrin, A.M. Tulgestke, L.T. Zaczek, D.F. Davidson, R.K. Hanson, Constrained reaction volume shock tube study of n-heptane oxidation: ignition delay times and time-histories of multiple species and temperature, *Proc. Combust. Inst.* 35 (2015) 231–239.